# Spin-orbit torque-induced switching in ferrimagnetic alloys: Experiments and modeling

Soong-Geun Je, Juan-Carlos Rojas-Sánchez, Thai Ha Pham, Pierre Vallobra, Gregory Malinowski, Daniel Lacour, Thibaud Fache, Marie-Claire Cyrille, Dae-Yun Kim, Sug-Bong Choe, Mohamed Belmeguenai, Michel Hehn, Stéphane Mangin, Gilles Gaudin, and Olivier Boulle

Citation: Appl. Phys. Lett. **112**, 062401 (2018); doi: 10.1063/1.5017738

View online: https://doi.org/10.1063/1.5017738

View Table of Contents: http://aip.scitation.org/toc/apl/112/6

Published by the American Institute of Physics

# Spin-orbit torque-induced switching in ferrimagnetic alloys: Experiments and modeling

Soong-Geun Je,[1,2,a)] Juan-Carlos Rojas-Sánchez,[2] Thai Ha Pham,[2] Pierre Vallobra,[2] Gregory Malinowski,[2] Daniel Lacour,[2] Thibaud Fache,[2] Marie-Claire Cyrille,[3] Dae-Yun Kim,[4] Sug-Bong Choe,[4] Mohamed Belmeguenai,[5] Michel Hehn,[2] Stéphane Mangin,[2] Gilles Gaudin,[1] and Olivier Boulle[1]

[1]*SPINTEC, University Grenoble Alpes, CEA, CNRS, Grenoble INP, INAC-Spintec, 38000 Grenoble, France*
[2]*Institut Jean Lamour, UMR 7198 CNRS-Université de Lorraine, 54506 Vandoeuvre lès Nancy, France*
[3]*CEA, LETI, MINATEC Campus, F-38054 Grenoble, France*
[4]*Department of Physics and Institute of Applied Physics, Seoul National University, Seoul 08826, South Korea*
[5]*LSPM (CNRS-UPR 3407), Université Paris 13, Sorbonne Paris Cité, 99 avenue Jean-Baptiste Clément, 93430 Villetaneuse, France*

(Received 29 November 2017; accepted 24 January 2018; published online 5 February 2018)

We investigate spin-orbit torque (SOT)-induced switching in rare-earth-transition metal ferrimagnetic alloys using W/CoTb bilayers. The switching current is found to vary continuously with the alloy concentration, and no reduction in the switching current is observed at the magnetic compensation point despite a very large SOT efficiency. A model based on coupled Landau-Lifschitz-Gilbert (LLG) equations shows that the switching current density scales with the effective perpendicular anisotropy which does not exhibit strong reduction at the magnetic compensation, explaining the behavior of the switching current density. This model also suggests that conventional SOT effective field measurements do not allow one to conclude whether the spins are transferred to one sublattice or just simply to the net magnetization. The effective spin Hall angle measurement shows an enhancement of the spin Hall angle with the Tb concentration which suggests an additional SOT contribution from the rare earth Tb atoms. *Published by AIP Publishing*. https://doi.org/10.1063/1.5017738

Current-induced spin-orbit torque (SOT) provides an efficient means of manipulating magnetization, paving the way for the next generation spintronic devices.[1,2] So far, intensive studies have focused on ferromagnetic materials combined with nonmagnetic heavy metals (HM) with strong spin-orbit coupling, which serve as a source of spin currents.[3–7] Recently, in the search for more efficient SOT switching, antiparallelly coupled magnetic systems, such as ferrimagnets and antiferromagnets, have attracted great interest[8–14] motivated by the anticipation of the low energy consumption in the switching,[15] as well as the immunity against external magnetic perturbation, which make those magnetic systems more promising as a data storage medium.[16]

Particularly, RE-TM ferrimagnetic alloys offer additional advantages. In the RE-TM alloys, where RE and TM sublattices are antiferromagnetically coupled, the net magnetic moment can be tuned easily by varying the RE-TM composition and temperature due to different concentrations and temperature dependences of the two sublattices.[17,18] As a result, the system can become either RE dominant (the net magnetization is along the RE magnetization direction) or TM dominant, and there exists the magnetic compensation point where the RE and TM magnetizations are cancelled out, resulting in zero net magnetization.

Due to the presence of the two antiferromagnetically coupled sublattices, such materials can be a model system to get insights into the spin transfer mechanism by studying how the SOT-related phenomena change depending on the chemical composition of RE-TM alloys.[9] Since the 4f orbitals, responsible for the magnetism of RE atoms, are generally far below the Fermi level, one might expect that TM atoms, rather than RE atoms, predominantly interact with the spin currents like the ferromagnetic materials. However, recent experiments on the SOT switching sign and the SOT effective field argued that the SOT acts on the net magnetization.[8–10] Particularly, a divergence of the effective field near the magnetization compensation point is reported,[8,12–14] leading to a huge effective field. However, no reduction of the threshold switching current density has been observed at the compensation,[8,14] unlike the expectation of the minimized current density in the case that the SOT was only acting on the net magnetization.[15] This apparent contradiction underlines a current lacunary understanding of the magnetization reversal by SOT in these systems.

In this work, we study the SOT switching current in CoTb ferrimagnetic alloys with an adjacent W layer. The SOT-induced switching is observed in a wide range of Co and Tb concentrations, even near the magnetic compensation point where a very large reversal field is needed ($\sim$1.3 T). When varying the alloy composition, the switching current density does not exhibit any reduction at the magnetic compensation, but instead a monotonous variation is observed. To explain these experimental results, we develop a simple model based on antiferromagnetically coupled Landau-Lifschitz-Gilbert (LLG) equations. The model shows that the threshold switching current density does not scale with the net magnetization but with the effective perpendicular

[a)]Present address: Center for X-ray Optics, Lawrence Berkeley National Laboratory, Berkeley, California 94720, USA and Department of Materials Science and Engineering, Korea University, Seoul 02481, South Korea. Electronic mail: soonggeun.je@gmail.com

anisotropy. The latter does not exhibit the compensating nature at the magnetic compensation, accounting for the absence of minimization of switching current at the compensation. The model also shows that conventional SOT effective field measurements cannot be the determinative method to conclude that the spin angular momentum is simply transferred to net magnetization, as claimed in previous works. Finally, using the domain wall (DW) motion based technique, the SOT effective field and the corresponding effective spin Hall angle are measured. We find that the effective spin Hall angle increases by a factor of 2 with the increasing Tb concentration, indicating an additional contribution of the Tb atoms to SOT.

For this study, a series of W(3 nm)/$Co_xTb_{1-x}$(3.5 nm)/Al (3 nm, naturally oxidized) films, which exhibit bulk perpendicular magnetic anisotropy, was grown by DC magnetron sputtering with x varying between x = 0.71 and x = 0.86 across the magnetic compensation. The films were then patterned into 20 $\mu$m-wide and 100 $\mu$m-long tracks with two Hall bars. Figure 1(a) shows an illustration of the sample structure and the measurement setup. Here, the W under layer serves as a spin current source to utilize the damping-like SOT.[19] The direction of magnetization is detected using the anomalous Hall effect (AHE). Since the magneto-transport properties are dominated by the 3d orbitals of TM, one can measure the magnetization of the TM sublattice even at the magnetic compensation point. The coercive field versus Co concentration x is plotted in Fig. 1(b). The divergence of the coercive field at x $\sim$ 0.77 (green dashed line) indicates that the magnetic compensation occurs around this region as is also confirmed by the sign reversal of AHE observed [Fig. 1(b)]. Magnetization switching induced by SOT was then performed by injecting in-plane current pulses of 3 ms in the Hall bars under a dc magnetic field in the direction of the current.[1] Figures 1(c) and 1(d) show typical examples of the AHE field hysteresis cycle and the switching, respectively. It is worth mentioning that the SOT-induced switching is achieved by a moderate current density ($\sim 10^{11}$ A/m$^2$) in this sample despite a very large coercive field of 1.3 T, suggesting a promising characteristic for memory applications. The SOT switching is observed in all alloy compositions, and Fig. 1(e) summarizes the switching current density $J_{sw}$ versus x. We note that the current density refers to the one flowing in the W layer. To determine this, the resistivity of a 3-nm thick W layer (162 $\mu\Omega$ cm) is taken into account. $J_{sw}$ shows a continuous behavior without any noticeable anomaly across the compensation, in contradiction with the expected reduction of $J_{sw}$ at the compensation point.[15]

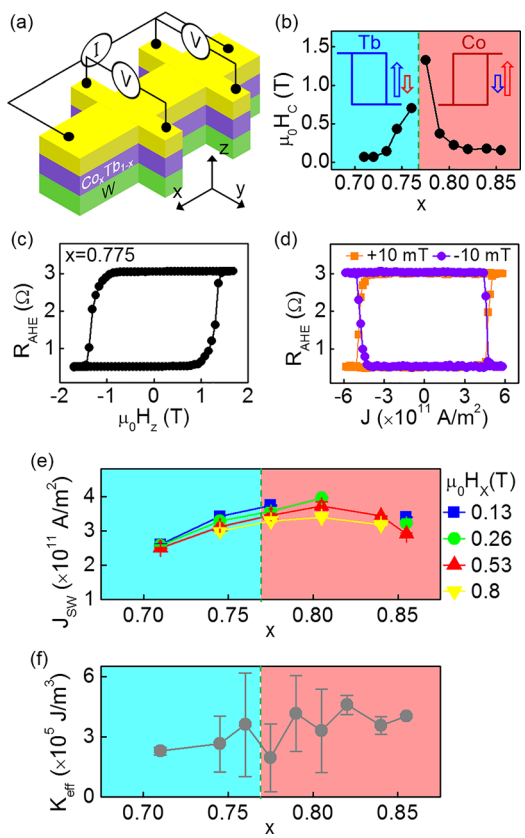


FIG. 1. (a) Schematic of the sample structure and AHE measurement. (b) The coercive field of the CoTb ferrimagnetic alloys versus the composition. The blue and red arrows stand for the Tb and Co magnetizations in the presence of $+\boldsymbol{H}_z$, respectively. The blue region (red region) stands for the Tb dominant phase (Co dominant phase). (c) Out-of-plane magnetization curve for a composition x = 0.775 close to the magnetic compensation point. (d) Current-induced magnetization switching at x = 0.775 ($|\mu_0 \boldsymbol{H}_x| = \pm 10$ mT). (e) Switching current density for various $\boldsymbol{H}_x$ values on the left (in T). (f) Effective anisotropy energy vs the alloy composition. The large error bars near the magnetic compensation point originate from the combination of large effective anisotropy fields and the uncertainty in measuring small **M**.

To understand the continuous change in $J_{sw}$, we consider a simple model where the magnetization dynamics in the alloy is described by two strongly antiferromagnetically coupled sublattices a and b, subjected to the SOT. The magnetization dynamics is described by modified LLG equations[20] including the damping-like SOT and a coupling term as

$$\frac{\dot{\boldsymbol{M}}^a}{\gamma^a} = -\boldsymbol{M}^a \times \mu_0(\boldsymbol{H}^{ext} + c\boldsymbol{M}^b) + \boldsymbol{M}^a \times \frac{\delta E^a_{ani}}{\delta \boldsymbol{M}^a} + \frac{\alpha^a}{M^a \gamma^a}\boldsymbol{M}^a \times \dot{\boldsymbol{M}}^a - pT^a \boldsymbol{M}^a \times (\hat{\boldsymbol{y}} \times \boldsymbol{m}^a), \quad (1a)$$

$$\frac{\dot{\boldsymbol{M}}^b}{\gamma^b} = -\boldsymbol{M}^b \times \mu_0(\boldsymbol{H}^{ext} + c\boldsymbol{M}^a) + \boldsymbol{M}^b \times \frac{\delta E^b_{ani}}{\delta \boldsymbol{M}^b} + \frac{\alpha^b}{M^b \gamma^b}\boldsymbol{M}^b \times \dot{\boldsymbol{M}}^b - qT^b \boldsymbol{M}^b \times (\hat{\boldsymbol{y}} \times \boldsymbol{m}^b). \quad (1b)$$

The sublattice a (b) is depicted by the magnitude $M^{a(b)}$ of its magnetization, the unit vector $\boldsymbol{m}^{a(b)} = \boldsymbol{M}^{a(b)}/M^{a(b)}$ with the gyromagnetic ratio $\gamma^{a(b)}$, and the damping constant $\alpha^{a(b)}$. The two equations are coupled by the local exchange field $c\boldsymbol{M}^{b(a)}$ so that $c\boldsymbol{M}^{b(a)}$ from the sublattice b (a) acts on the sublattice a (b) with the coupling constant $c$. $\boldsymbol{H}^{ext}$ is the external field, and $E^{a(b)}_{ani}$ is the effective anisotropy energy, which includes the magnetocrystalline anisotropy energy and the demagnetizing energy. The last term is the damping-like torque (spin-Hall torque), which is characterized by $T^{a(b)} = \hbar\theta^{eff}_{SH} J/2eM^{a(b)}t$, where $\hbar$ is the reduced Planck constant, $\theta^{eff}_{SH}$ is the effective spin Hall angle, $J$ is the charge current density through the heavy metal layer, $e$ is the electron charge, and $t$ is the thickness of the magnetic layer. Here, $p$ and $q$ denote weighting factors for the transfer of the spin current to the sublattices a and b, respectively, so that we take into account the element dependent absorption rate of

each sublattice. Since we are assuming that the incoming spin angular momentum is fully transferred to the magnetic layer, the sum of $p$ and $q$ should equal 1. Strongly coupled antiparallel sublattices are also assumed, and thus, the net magnetization is $\boldsymbol{M} = M\boldsymbol{m}$, where $M = M^a - M^b$ and the unit vector $\boldsymbol{m} = \boldsymbol{m}^a = -\boldsymbol{m}^b$.

After substituting $\boldsymbol{m}^{a(b)}$ with $\boldsymbol{m}$ and summing up Eqs. (1a) and (1b), one obtains

$$\dot{\boldsymbol{m}} = -\mu_0\gamma_{eff}\boldsymbol{m}\times\boldsymbol{H}^{ext} + \frac{\gamma_{eff}}{M}\boldsymbol{m}\times\left(\frac{\delta E_{ani}}{\delta \boldsymbol{m}}\right) + \alpha_{eff}\boldsymbol{m} \times \dot{\boldsymbol{m}} - \gamma_{eff}(p+q)\left(\frac{\hbar\theta_{SH}^{eff}}{2e\mathrm{M}t}\right)J\boldsymbol{m}\times(\hat{\boldsymbol{y}}\times\boldsymbol{m}), \quad (2)$$

where $E_{ani} = m_z^2 K_{eff}$ with the total effective anisotropy $K_{eff} = K - \frac{\mu_0(M_a - M_b)^2}{2}$, the effective values of the gyromagnetic ratio $\gamma_{eff} = (M^a - M^b)/\left(\frac{M^a}{\gamma^a} - \frac{M^b}{\gamma^b}\right)$, and the effective damping constant $\alpha_{eff} = \left(\frac{\alpha^a M^a}{\gamma^a} + \frac{\alpha^b M^b}{\gamma^b}\right)/\left(\frac{M^a}{\gamma^a} - \frac{M^b}{\gamma^b}\right)$. Note that all terms are written in terms of the net magnetization and the weighting factors disappear in the final form, as $p + q = 1$.

By solving Eq. (2) and following Ref. 21, the switching current density of the ferrimagnetic system is obtained as $J_{sw} \approx \frac{2e}{\hbar}\frac{t}{\theta_{SH}^{eff}}\left(K_{eff} - \frac{\mu_0 H_x M}{\sqrt{2}}\right)$, where $H_x$ is an in-plane field along the current to facilitate the deterministic SOT switching. In our experiments, the first term proportional to $K_{eff}$ is much larger than the second term. Thus, $J_{sw}$ does not scale linearly with $M$ but scales with the net $K_{eff}$. Since the net $K_{eff}$ is obtained from the sum of effective anisotropy energy values of each lattice, $K_{eff}$ is not cancelled out. The $M$ dependence of $J_{sw}$ arises from the demagnetizing energy in the effective anisotropy as and the Zeeman term with the in-plane magnetic field. As a result, no large reduction of the critical current density is predicted at the compensation. Therefore, the switching current density in the antiferromagnetically coupled system exhibits the continuous behavior, rather than the drastic change, across the compensation point.[8,14,22]

Figure 1(f) shows the $K_{eff}$ of the W/Co$_x$Tb$_{1-x}$ alloys versus x. $K_{eff}$ is determined by $M$ and the effective anisotropy field, which is obtained by the tilting of the magnetization under rotating external fields of 0.5–2 T. The tilting is measured using AHE, and the effective anisotropy field is then extracted by the best fit formulated by the Stoner-Wohlfarth model.[23] $K_{eff}$ changes continuously across the magnetic compensation, which is a similar trend to the switching current density as shown in Fig. 1(e). Thus, the dependence of $K_{eff}$ on the alloy concentration can explain the absence of a reduction of the switching current density observed experimentally. The small dip in $K_{eff}$ near the compensation can be explained by the limit of the simple Stoner-Wohlfarth model, which does not consider the small misalignment of the Tb and Co sublattices due to the large magnetic field needed to tilt magnetization, as discussed in previous reports.[24,25] Note that our model is based on the macrospin model and the heating effect is not considered. Recent studies have shown that the magnetization switching occurs in more complex manners,[26,27] for example, the DW creation and propagation, and the thermal effect plays an important role.[22]

We then measure the SOT-induced effective field by measuring the modulation of the DW dynamics induced by SOT.[28–30] The measurement scheme and typical AHE resistance data are presented in Fig. 2(a). The DW is driven by a perpendicular magnetic field $H_z$ under a small bias DC current, and the DW motion is monitored at each Hall bar in real time. The two AHE resistance data set then gives us the time ($t$) taken passing each Hall cross of length $L$ and the DW propagation direction. Figure 2(b) shows the DW velocity $v(= L/t)$ as a function of $\mu_0 H_z$ under opposite bias currents. The two curves are shifted horizontally by $\pm H_z^{eff}$. Thus, the SOT-induced effective field for a given current density $J$ acts on the DW like an effective field $H_z^{eff}$. The linear relationship between $H_z^{eff}$ and current density $J$ [Fig. 2(c)] allows us to extract the efficiency of the SOT, defined as $\chi \equiv H_z^{eff}/J$. In these measurements, a very low current density regime ($<1.5\times10^{10}$ A/m$^2$) was used to minimize the heating effect. Indeed, for larger current densities, we observe that the effective field deviates from the linear relationship, which yields the overestimation or underestimation of $\chi$ as shown in the inset of Fig. 2(c). $\chi$ is measured with respect to an in-plane field $H_x$, as typically shown in Fig. 2(d) for Tb dominant and Fig. 2(e) for Co dominant, which gives the DW configuration dependence of the effective field. $\chi$ increases linearly with $H_x$ up to $H_{sat}$ where it stays at a constant value $\chi_{sat}$.

Figure 3(a) shows the SOT efficiency $\chi_{sat}$ with various compositions. $\chi_{sat}$ diverges significantly as approaching the

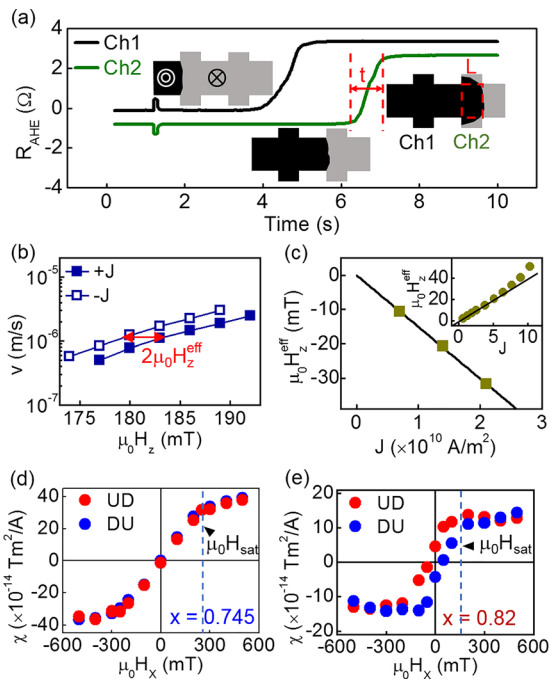


FIG. 2. (a) Schematic of the DW velocity measurement for the effective field measurement. The DW is nucleated at a natural nucleation point by a pulsed magnetic field. To eliminate the case where the DW is nucleated between the Hall bars, the data that exhibit sufficiently separated reversal times are taken. (b) Typical example of DW speed curves (x = 0.82 at $\mu_0 H_x = 0.3$ T) modulated by $\mu_0 H_z^{eff}$. Here, the dc current density is $\pm 1.59\times10^{10}$ A/m$^2$. (c) Current-induced effective field as a function of current density (x = 0.82 at $\mu_0 H_x = -0.3$ T). (Inset) Deviation of the effective field from linearity for large current densities (x = 0.745). (d) and (e) Typical examples of the efficiency $\chi(\mu_0 H_x)$ for Tb-dominant (d) and Co-dominant (e) alloys. The UD (DU) refers to the up domain (down domain) expansion.

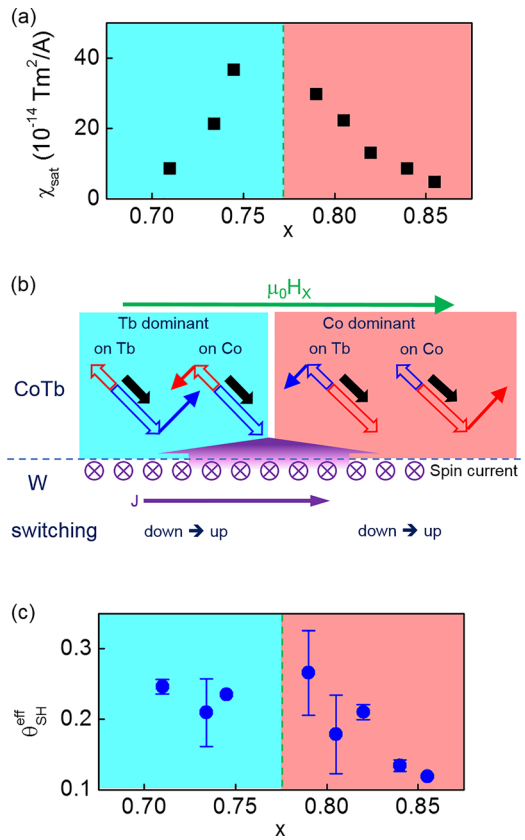


FIG. 3. (a) Divergence of $\chi_{sat}$ near the magnetic compensation. (b) Schematic representation of SOT effective fields (blue and red solid arrows) acting on the Tb (blue hollow arrow) and Co (red hollow arrow) magnetizations. The spin current is transferred from the W layer and exerts a torque on either only Tb or only Co sublattices. In any case, the resultant switching polarity is the same [the same switching sign of the net magnetization (black arrows)]. (c) Effective spin Hall angle as a function of x.

magnetic compensation point, indicating the $1/M$ dependence. The magnitude reaches up to $37 \times 10^{-14}\,\mathrm{T\,m^2/A}$. We note that this value is more than 3 times larger than in Ta/CoTb ferrimagnetic alloys[8] and 5 times larger compared to the ferromagnetic Pt/Co/AlOx trilayers.[3] Although the effective field is found to be extremely large at the compensation point, we note that this is not indicative of the significantly efficient switching operation. For the switching operation, it is important to overcome the energy barrier,[21,26] which is dominated by the effective anisotropy energy. However, since the effective anisotropy does not simply scale as $M$, the minimized magnetization does not lead to the minimization of the switching current, which is more relevant to the device operation in terms of energy consumption.

To analyze these results, we consider a collective coordinate model which assumes the static DW structure during its motion, and the DW is described by its position $q$ and the DW angle $\psi$.[31,32] Using the coupled LLG equations and a Lagrangian approach,[32–34] one obtains the following coupled equations

$$\dot{\psi} + \alpha_{eff}\frac{\dot{q}}{\Delta} = \gamma_{eff} J(p+q)\frac{\pi}{2}\frac{\hbar\theta_{SH}^{eff}}{2eMt}\sin\psi + \mu_0\gamma_{eff}H_z$$
$$\alpha_{eff}\dot{\psi} - \frac{\dot{q}}{\Delta} = \mu_0\gamma_{eff}\frac{\pi}{2}H_x\cos\psi - \mu_0\gamma_{eff}\frac{M\mathrm{N_{DW}}\sin 2\psi}{2}, \quad (3)$$

where $\Delta = \sqrt{\frac{A}{K_{eff}}}$ and $\mathrm{N_{DW}} = \frac{t\ln 2}{\pi\Delta}$.[35]

We neglect here the Dzyaloshinskii-Moryia interaction (DMI, which will be discussed later). From this equation, one sees that the SOT term is equivalent to an effective field $\mu_0 H_{SOT}^{eff} = J(p+q)\frac{\pi}{2}\frac{\hbar\theta_{SH}^{eff}}{2eMt}\sin\psi$. For $H_x < H_{sat}$, the domain wall configuration continuously rotates from Bloch to Néel configurations so that $\sin\psi = \frac{2\pi H_x}{MN_{DW}}$ and $\chi$ scales linearly with $H_x$ as is observed experimentally. For $H_x > H_{sat}$, a Néel DW ($\psi = \frac{\pi}{2}$) is achieved, which leads to a saturation efficiency $\chi_{sat} = \frac{H_{SOT}^{eff}}{J} = (p+q)\frac{\pi}{2}\frac{\hbar\theta_{SH}^{eff}}{2eMt}$. Note that a similar expression for the effective field and particularly the $1/M$ dependence can also be derived from the LLG equation [Eq. (2)].[36] As mentioned above, since the sum of the weighting factors is 1, the detailed sublattice dependence disappears and $H_{SOT}^{eff}$ simply carries the net magnetization like the ferromagnetic case. Thus, the SOT effective field in ferrimagnets diverges at the magnetic compensation point,[8,12–14] like the divergence of the magnetic coercive field. Note that the effective field is basically determined by the comparison between the effect of the SOT transferred, which does not depend on $M$, and the magnetic susceptibility to an external field, and so, even though the same torque is transferred to the magnetic system, the system with small $M$ gives rise to the larger effective field.

We also note that the divergent behavior, the sign of the effective field, and the switching polarity cannot be the proof that the SOT acts on the net magnetization rather than the TM sublattice.[10,13] Even in the case that the angular momentum absorption into one sublattice is completely turned off, i.e., either $p$ or $q$ is 0, the experimentally determined effective field and switching current always show the same behavior and the same switching sign due to the strong coupling as illustrated in Fig. 3(b).

To characterize the variation of the SOT on the material composition, a more relevant parameter is the effective spin Hall angle $\theta_{SH}^{eff}$, which stands for how much spin currents are transmitted to a magnetic layer. Figure 3(c) shows $\theta_{SH}^{eff}$ of W/$\mathrm{Co_xTb_{1-x}}$ alloys vs x. The values range from 0.11 to 0.26, reflecting the giant spin Hall angle of $\beta$-W.[4,6,19] Interestingly, there is a noticeable increase in $\theta_{SH}^{eff}$, by a factor of 2, when passing from the Co rich to the Tb rich phases. The increasing $\theta_{SH}^{eff}$ with the Tb concentration might indicate an additional contribution from the Tb atoms which have a large orbital angular momentum, and recent reports have shown that the RE atoms give rise to SOT in RE/FM heterostructures.[37,38] Although our films are alloys, it is reported that a segregation in the Tb composition, which is pronounced for low thickness, can occur and result in a relatively Tb-rich region at the top of the magnetic layer.[39,40] Since the sign of the spin Hall angle of RE is found to be positive,[37] the spin currents from the bottom W and relatively rich Tb region at the top can be additive, thereby enhancing $\theta_{SH}^{eff}$ as the Tb concentration increases. Alternatively, this can be ascribed to the increase in transparency of the W/CoTb interface due to the increasing Tb composition, which may alter the interface properties, such as the spin-mixing conductance and hence $\theta_{SH}^{eff}$.[41]

Finally, since the DW motion based SOT effective field measurement is performed on a single DW, this technique

enables us to quantify the DMI-induced effective field.[26–28] However, we find no significant DMI-induced field in the W/$Co_xTb_{1-x}$ system which might be attributed to the relatively thick magnetic layer (3.5 nm) and the single interface. The field-driven method[42,43] and the Brillouin light scattering method[44] also yield consistent results.

To conclude, we investigated the SOT-induced switching in RE-TM ferrimagnetic alloys. We find that the switching current density exhibits continuous behavior without a notable reduction in the vicinity of the magnetic compensation point. According to the simple model based on antiferromagnetically coupled LLG equations, we find that the switching current density scales with the effective anisotropy, which exhibits no reduction at the magnetic compensation, elucidating the continuous behavior of the switching current density. In the model, we also note that conventional SOT effective field measurement cannot answer the question of whether the spin currents are absorbed into one particular sublattice or the net magnetization. The effective spin Hall angle measurement shows an enhancement of the spin Hall angle with the Tb concentration which might suggest an additional SOT contribution from the rare earth Tb atoms. Our results provide insights into the SOT-induced switching phenomena in the antiferromagnetically coupled system, which are promising for future spintronic devices.

This work was supported by the project ICEEL INTERCARNOT OPTICSWITCH. S.G.J. was partially supported by the Leading Foreign Research Institute Recruitment Program through the National Research Foundation (NRF) of Korea funded by the Ministry of Education, Science and Technology (MEST) (2012K1A4A3053565) and by the DGIST R&D program of the Ministry of Science, ICT and future Planning (17-BT-02). D.Y.K. and S.B.C. were supported by grants from NRF funded by the Ministry of Science, ICT and Future Planning of Korea (MSIP) (2015R1A2A1A05001698 and 2015M3D1A1070465). S.G.J also acknowledges the support from the Future Materials Discovery Program through the NRF funded by the MSIP (2015M3D1A1070465).

[1]I. M. Miron, K. Garello, G. Gaudin, P.-J. Zermatten, M. V. Costache, S. Auffret, S. Bandiera, B. Rodmacq, A. Schuhl, and P. Gambardella, Nature **476**, 189–193 (2011).
[2]L. Liu, O. J. Lee, T. J. Gudmundsen, D. C. Ralph, and R. A. Buhrman, Phys. Rev. Lett. **109**, 096602 (2012).
[3]K. Garello, I. M. Miron, C. O. Avci, F. Freimuth, Y. Mokrousov, S. Blugel, S. Auffret, O. Boulle, G. Gaudin, and P. Gambardella, Nat. Nanotechnol. **8**, 587 (2013).
[4]L. Liu, C.-F. Pai, Y. Li, H. W. Tseng, D. C. Ralph, and R. A. Buhrman, Science **336**, 555 (2012).
[5]S. Woo, M. Mann, A. J. Tan, L. Caretta, and G. S. D. Beach, Appl. Phys. Lett. **105**, 212404 (2014).
[6]Q. Hao and G. Xiao, Phys. Rev. Appl. **3**, 034009 (2015).
[7]M. Cubukcu, O. Boulle, M. Drouard, K. Garello, C. O. Avci, I. M. Miron, J. Langer, B. Ocker, P. Gambardella, and G. Gaudin, Appl. Phys. Lett. **104**, 042406 (2014).
[8]J. Finley and L. Liu, Phys. Rev. Appl. **6**, 054001 (2016).
[9]N. Roschewsky, T. Matsumura, S. Cheema, F. Hellman, T. Kato, S. Iwata, and S. Salahuddin, Appl. Phys. Lett. **109**, 112403 (2016).
[10]K. Ueda, M. Mann, C.-F. Pai, A.-J. Tan, and G. S. D. Beach, Appl. Phys. Lett. **109**, 232403 (2016).
[11]Z. Zhao, M. Jamali, A. K. Smith, and J.-P. Wang, Appl. Phys. Lett. **106**, 132404 (2015).
[12]N. Roschewsky, C.-H. Lambert, and S. Salahuddin, Phys. Rev. B **96**, 064406 (2017).
[13]W. S. Ham, S. Kim, D.-H. Kim, K.-J. Kim, T. Okuno, H. Yoshikawa, A. Tsukamoto, T. Moriyama, and T. Ono, Appl. Phys. Lett. **110**, 242405 (2017).
[14]R. Mishra, J. Yu, X. Qiu, M. Motapothula, T. Venkatesan, and H. Yang, Phys. Rev. Lett. **118**, 167201 (2017).
[15]J. Z. Sun and D. C. Ralph, J. Magn. Magn. Mater. **320**, 1227 (2008).
[16]T. Jungwirth, X. Marti, P. Wadley, and J. Wunderlich, Nat. Nanotechnol. **11**, 231 (2016).
[17]M. Gottwald, M. Hehn, F. Montaigne, D. Lacour, G. Lengaigne, S. Suire, and S. Mangin, J. Appl. Phys. **111**(8), 083904 (2012).
[18]R. Tolley, T. Liu, Y. Xu, S. Le Gall, M. Gottwald, T. Hauet, M. Hehn, F. Montaigne, E. E. Fullerton, and S. Mangin, Appl. Phys. Lett. **106**(24), 242403 (2015).
[19]C.-F. Pai, L. Liu, Y. Li, H. W. Tseng, D. C. Ralph, and R. A. Buhrman, Appl. Phys. Lett. **101**, 122404 (2012).
[20]H. Oezelt, A. Kovacs, F. Reichel, J. Fischbacher, S. Bance, M. Gusenbauer, C. Schubert, M. Albrecht, and T. Schrefl, J. Magn. Magn. Mater. **381**, 28 (2015).
[21]K.-S. Lee, S.-W. Lee, B.-C. Min, and K.-J. Lee, Appl. Phys. Lett. **102**, 112410 (2013).
[22]T.-H. Pham, S.-G. Je, P. Vallobra, T. Fache, D. Lacour, G. Malinowski, M. C. Cyrille, G. Gaudin, O. Boulle, M. Hehn *et al.*, e-print arXiv:1711.10790.
[23]K.-W. Moon, J.-C. Lee, S.-B. Choe, and K.-H. Shin, Rev. Sci. Instrum. **80**, 113904 (2009).
[24]F. Hellman, Appl. Phys. Lett. **59**, 2757 (1991).
[25]T. Wu, H. Fu, R. A. Hajjar, T. Suzuki, and M. Mansuripur, J. Appl. Phys. **73**, 1368 (1993).
[26]N. Mikuszeit, O. Boulle, I. M. Miron, K. Garello, P. Gambardella, G. Gaudin, and L. D. Buda-Prejbeanu, Phys. Rev. B **92**, 144424 (2015).
[27]O. J. Lee, L. Q. Liu, C. F. Pai, Y. Li, H. W. Tseng, P. G. Gowtham, J. P. Park, D. C. Ralph, and R. A. Buhrman, Phys. Rev. B **89**, 024418 (2014).
[28]S.-G. Je, S.-C. Yoo, J.-S. Kim, Y.-K. Park, M.-H. Park, J. Moon, B.-C. Min, and S.-B. Choe, Phys. Rev. Lett. **118**, 167205 (2017).
[29]J. H. Franken, M. Herps, H. J. M. Swagten, and B. Koopmans, Sci. Rep. **4**, 5248 (2014).
[30]S. Emori, E. Martinez, K.-J. Lee, H.-W. Lee, U. Bauer, S.-M. Ahn, P. Agrawal, D. C. Bono, and G. S. D. Beach, Phys. Rev. B **90**, 184427 (2014).
[31]A. Malozemoff and J. Slonczewski, *Magnetic Domain Walls in Bubble Materials* (Academic Press, New York, 1979).
[32]A. Hubert, *Theorie der Domänenwände in Geordneten Medien* (Springer, Berlin, 1974).
[33]A. Thiaville, S. Rohart, É. Jué, V. Cros, and A. Fert, Europhys. Lett. **100**, 57002 (2012).
[34]O. Boulle, S. Rohart, L. D. Buda-Prejbeanu, E. Jué, I. M. Miron, S. Pizzini, J. Vogel, G. Gaudin, and A. Thiaville, Phys. Rev. Lett. **111**, 217203 (2013).
[35]S. V. Tarasenko, A. Stankiewicz, V. V. Tarasenko, and J. Ferré, J. Magn. Magn. Mater. **189**, 19 (1998).
[36]T. Schulz, K. Lee, B. Krüger, R. L. Conte, G. V. Karnad, K. Garcia, L. Vila, B. Ocker, D. Ravelosona, and M. Kläui, Phys. Rev. B **95**, 224409 (2017).
[37]N. Reynolds, P. Jadaun, J. T. Heron, C. L. Jermain, J. Gibbons, R. Collette, R. A. Buhrman, D. G. Schlom, and D. C. Ralph, Phys. Rev. B **95**(6), 064412 (2017).
[38]K. Ueda, C.-F. Pai, A. J. Tan, M. Mann, and G. S. D. Beach, Appl. Phys. Lett. **108**, 232405 (2016).
[39]B. Hebler, A. Hassdenteufe, P. Reinhard, H. Karl, and M. Albrecht, Front. Mater. **3**, 8 (2016).
[40]M. S. E. Hadri, M. Hehn, P. Pirro, C.-H. Lambert, G. Malinowski, E. E. Fullerton, and S. Mangin, Phys. Rev. B **94**, 064419 (2016).
[41]C.-F. Pai, Y. Ou, L. Henrique Vilela-Leão, D. C. Ralph, and R. A. Buhrman, Phys. Rev. B **92**, 064426 (2015).
[42]S.-G. Je, D.-H. Kim, S.-C. Yoo, B.-C. Min, K.-J. Lee, and S.-B. Choe, Phys. Rev. B **88**, 214401 (2013).
[43]D.-Y. Kim, M.-H. Park, Y.-K. Park, J.-S. Kim, Y.-S. Nam, D.-H. Kim, S.-G. Je, B.-C. Min, and S.-B. Choe, NPG ASIA Mater. **10**, e464 (2018).
[44]M. Belmeguenai, J.-P. Adam, Y. Roussigné, S. Eimer, T. Devolder, J.-V. Kim, S. M. Cherif, A. Stashkevich, and A. Thiaville, Phys. Rev. B **91**, 180405(R) (2015).